ELSEVIER

Journal of Nuclear Materials 246 (1997) 196–205

journal of nuclear materials

# Creep rupture properties of a Ni–Cr–W superalloy in air environment

Yuji Kurata [a,*], Hirokazu Tsuji [a], Masami Shindo [b], Hajime Nakajima [a]

[a] *Department of Materials Science and Engineering, Tokai Research Establishment, Japan Atomic Energy Research Institute, Tokai-mura, Naka-gun, Ibaraki-ken 319-11, Japan*

[b] *Office of planning, Tokai Research Establishment, Japan Atomic Energy Research Institute, Tokai-mura, Naka-gun, Ibaraki-ken 319-11, Japan*

Received 30 January 1997; accepted 20 April 1997

**Abstract**

The creep rupture properties in air environment were studied at 900, 1000 and 1050°C for bar, plate and seamless tube materials of a Ni–Cr–W superalloy developed for use at service temperatures around 1000°C. The long-term creep rupture strength is estimated by applying the time–temperature parameter method to the creep rupture data. Data of anomalous behaviour due to oxidation strengthening, which is observed in creep curves with rupture times above ~ 10 000 h at 1000°C, are corrected for the application of the time–temperature parameter method. The Larson–Miller parameter method is better than the Orr–Sherby–Dorn parameter method in respect of curve fitting to the present creep rupture data. The creep rupture strength of the bar material with grain sizes above ASTM No. 2 and of the plate material is above 9.8 MPa for a $1 \times 10^5$ h life at 1000°C, which is the final target of this program. The creep rupture strength increases with increasing grain size and heat treatment temperature. © 1997 Elsevier Science B.V.

## 1. Introduction

High temperature gas-cooled reactors (HTGRs) have excellent characteristics such as the supply of high temperature heat as high as 1000°C and high inherent safety. The high temperature engineering test reactor (HTTR) is under construction at the Japan Atomic Energy Research Institute (JAERI) to establish and upgrade HTGR technologies and carry out advanced basic research on high temperature technologies [1]. The HTTR is a test reactor with a thermal output of 30 MW and an outlet coolant temperature of 850°C at the rated operation and 950°C at the high temperature test operation. Hastelloy XR, a modified version of Hastelloy X is used as a high-temperature component material of an intermediate heat exchanger of the HTTR.

From the viewpoint of efficient use of nuclear heat energy and attainment of high heat efficiency, higher temperatures of the reactor outlet coolant are advantageous. However, the development of a new superalloy is indispensable to use metallic materials at temperatures above 950°C. Ni–Cr–W superalloys were recognized as one of the best materials for intermediate heat exchangers in the national research project concerning nuclear steelmaking in Japan, where some superalloys possessing high creep strength were developed [2–4]. In JAERI, study on the material behaviour in a HTGR system was carried out and, as a result, Hastelloy XR possessing a high corrosion resistance in a HTGR helium environment was developed [5]. Succeeding these research activities, the research and development of new heavy duty Ni–Cr–W superalloys for use at service temperatures around 1000°C have been promoted by JAERI in cooperation with experienced authorities of industrial and academic organizations [6–8].

The program had set the following targets:

(1) A creep rupture strength over 7.8 MPa for a $1 \times 10^5$ h life at 1000°C, with the final target being 9.8 MPa for the same life and temperature.

(2) No substantial susceptibility to intergranular attack or internal oxidation after exposure to the simulated HTGR helium at 1000°C for $1 \times 10^5$ h.

* Corresponding author. Tel.: +81-29 282 6472; fax: +81-29 282 5922; e-mail: kurata@jmpdsun.tokai.jaeri.go.jp.

0022-3115/97/$17.00 
*PII* S0022-3115(97)00106-2

Table 1
Chemical composition of an industrial scale Ni–Cr–W alloy (mass%)

| C | Si | Mn | P | S | Cr | W | Ti | Zr | Y | B | Co | Al | N | O | Fe | Nb | Ni |
|---|---|---|---|---|---|---|---|---|---|---|---|---|---|---|---|---|---|
| 0.029 | 0.06 | 0.02 | 0.003 | 0.001 | 18.76 | 21.43 | 0.06 | 0.02 | 0.008 | 0.006 | 0.02 | 0.04 | 0.0011 | 0.0005 | 0.07 | 0.02 | Bal. |

(3) Formability to 32 mm outer diameter, 4 to 5 mm thick, 7 m long seamless tubes.

(4) Enough capacity for the secondary cold-forming and welding.

The optimum chemical composition of the base metal, which can be expected to attain the targets of creep rupture strength and corrosion resistance, has been already proposed as a result of a series of experiments in this program [7]. Furthermore, it was shown that the Ni–Cr–W superalloy fabricated on an industrial scale possessed sufficient formability to seamless tubes [9]. One of the items to be solved in order to put the developed Ni–Cr–W superalloy to practical use is the estimation of long-term creep rupture strength.

In this paper, we studied the creep properties of bars, plates and tubes of the Ni–Cr–W alloy fabricated on an industrial scale and estimated creep rupture strength for a $1 \times 10^5$ h life at 1000°C.

## 2. Experimental procedure

### 2.1. Specimens

The material tested in this study is a Ni–Cr–W alloy manufactured on an industrial scale, i.e. 2000 kg. This alloy was developed for HTGRs with coolant outlet temperatures of around 1000°C and as longer life materials than Hastelloy XR used for the HTTR. Table 1 shows the chemical composition of this alloy. The main chemical composition of the alloy is Ni–18 to 19 mass% Cr–20 to 22 mass% W and the amounts of elements such as C, Mn, Si, Nb, Fe, B, Y and Ti are optimized. Product forms are round bars, plates and seamless tubes. Heat treatment shown in Table 2 was performed on bars to investigate the effect of heat treatment on creep properties. Heat treatments A, C and D are solution heat treatment and the grain size varies from ASTM No. 3 to 0. $\alpha_2$-W phase precipitated preferentially at grain boundaries in heat treatment B which was performed to obtain a fatigue resistant material. The plates were heat-treated at 1225°C for 1 h and this was followed by water cooling to obtain grain size No. 2. The solution heat treatment at 1230–1240°C was performed on tubes to obtain grain size No. 2–3 [9]. The specimens for creep tests were 6 mm in diameter and 30 mm in gauge length.

Table 2
Heat treatment condition and grain size for bars of a Ni–Cr–W alloy

| | Heat treatment condition | Grain size |
|---|---|---|
| A | 1215°C for 1 h WQ | ASTM No. 3 |
| B | 1215°C for 1 h WQ and 1190°C for 2 h AC | ASTM No. 3 |
| C | 1250°C for 1 h WQ | ASTM No. 2 |
| D | 1275°C for 1 h WQ | ASTM No. 0 |

### 2.2. Creep tests

Constant load creep tests in air were carried out at 900, 1000 and 1050°C for specimens sampled from bars with heat treatments A to D, plates and tubes. Four stress levels were employed for each temperature at 900 and 1000°C. The test under the lowest stress at each temperature was the creep deformation test until rupture and the other three tests at each temperature were creep-rupture tests. Tests under three stress levels were carried out at 1050°C. Creep tests at 900 and 1000°C were conducted at the National Research Institute for Metals and creep tests at 1050°C were conducted at the Tokyo Institute of Technology under contract with JAERI.

Microstructure observations were made for creep-ruptured specimens using an optical microscope and a scanning electron microscope.

## 3. Results and discussion

### 3.1. Creep test results

Fig. 1 shows the relationship between stress and time to rupture for specimens with heat treatments A to D. Al-

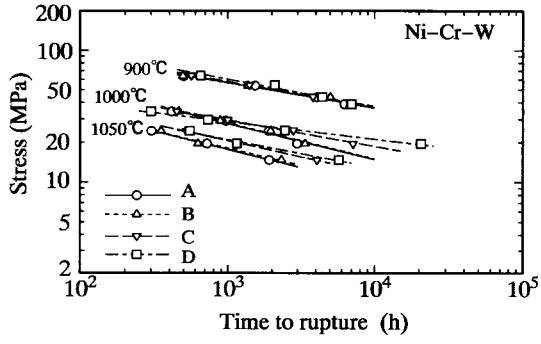


Fig. 1. Stress versus time to rupture in air for a Ni–Cr–W alloy with heat treatments A to D.

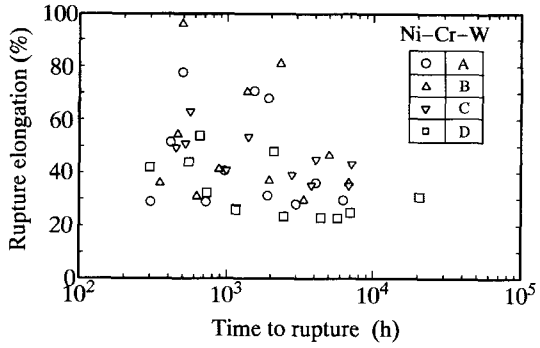


Fig. 2. Rupture elongation versus time to rupture in air for a Ni–Cr–W alloy with heat treatments A to D.

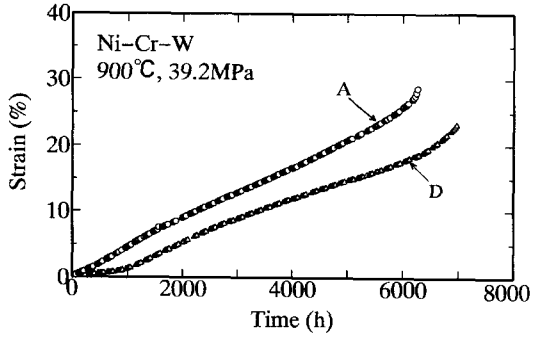


Fig. 3. Creep curves at 900°C under 39.2 MPa in air for a Ni–Cr–W alloy with heat treatment A and with heat treatment D.

though time to rupture at 900°C is almost independent of heat treatment, that for the specimen with high heat treatment temperature and large grain size becomes long at 1000 and 1050°C. A significant difference in time to rupture for the specimen between heat treatment A and B is not found. Rupture elongation versus time to rupture is plotted in Fig. 2. The values of rupture elongation for specimens with heat treatments A to D are above 20%.

Examples of creep curves at 900, 1000 and 1050°C are

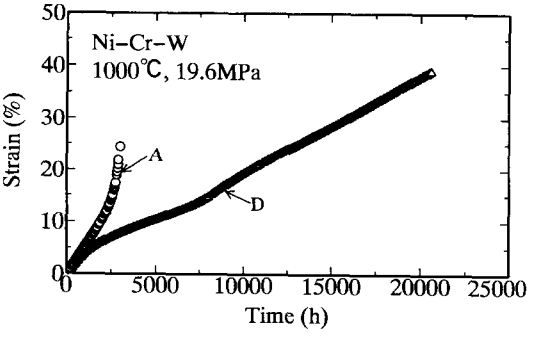


Fig. 4. Creep curves at 1000°C under 19.6 MPa in air for a Ni–Cr–W alloy with heat treatment A and with heat treatment D.

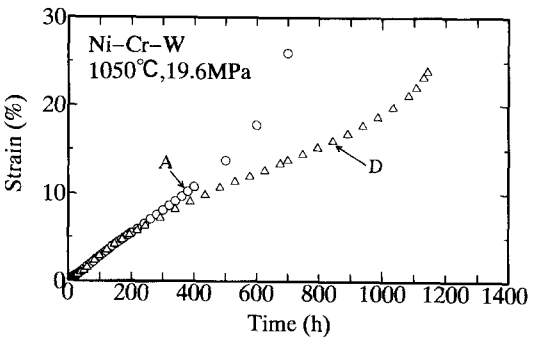


Fig. 5. Creep curves at 1050°C under 19.6 MPa in air for a Ni–Cr–W alloy with heat treatment A and with heat treatment D.

shown in Figs. 3–5, respectively. Although normal or classical type creep curves consisting of primary, secondary and tertiary creep stages are usually observed for pure metals, non-classical type creep curves are also observed for this alloy with large grain size. Two types of non-classical creep curves are observed for this Ni–Cr–W alloy. The first one has a region with a minimum creep rate preceding the primary creep stage as shown in the

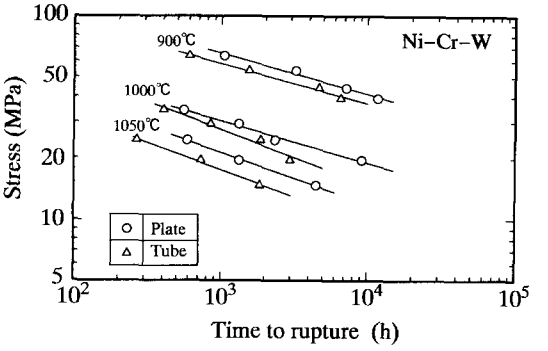


Fig. 6. Stress versus time to rupture in air for a Ni–Cr–W alloy sampled from plates and from tubes.

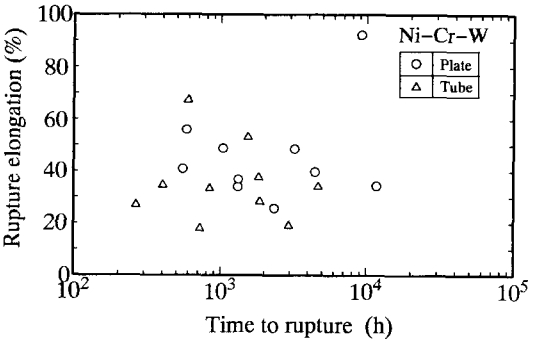


Fig. 7. Rupture elongation versus time to rupture in air for a Ni–Cr–W alloy sampled from plates and from tubes.

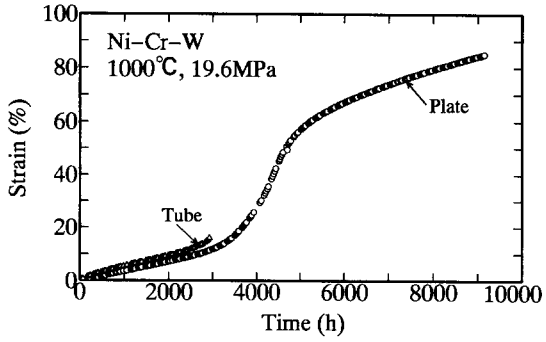


Fig. 8. Creep curves at 1000°C under 19.6 MPa in air for a Ni–Cr–W alloy sampled from plates and from tubes.

creep curve for heat treatment D of Fig. 3. The second one has a decreasing creep rate region after the tertiary creep stage as shown in the creep curve for heat treatment D of Fig. 4. In the latter case, anomalous behaviour where the creep rupture life is much longer than that expected from normal creep behaviour is observed. The cause of non-classical type creep curves found in this alloy is discussed later.

Fig. 6 shows the relationship between stress and time to rupture for specimens sampled from plates and tubes. The time to rupture for plates is longer than that for tubes. We think that this difference in rupture lives is caused by the difference in product process between plates and tubes. Rupture elongation versus time to rupture for specimens sampled from plates and tubes is also plotted in Fig. 7.

Creep curves at 1000°C under 19.6 MPa for specimens sampled from plates and tubes are shown in Fig. 8. While the creep curve for tubes is a normal type, that for plates is a non-classical type similar to that for heat treatment D of Fig. 4. In the creep curve for plates, the specimen suddenly ruptures during decreasing and steady-state creep rate stages after the tertiary creep stage.

### 3.2. Microstructure observation of creep-rupture specimens

Fig. 9(a) and (b) shows the appearance of specimens with heat treatments B and C after creep-rupture at 900°C under 39.2 MPa. The specimen shown in Fig. 9(c) came to pieces during removal from the creep testing machine after creep-rupture at 1000°C under 19.6 MPa. This specimen

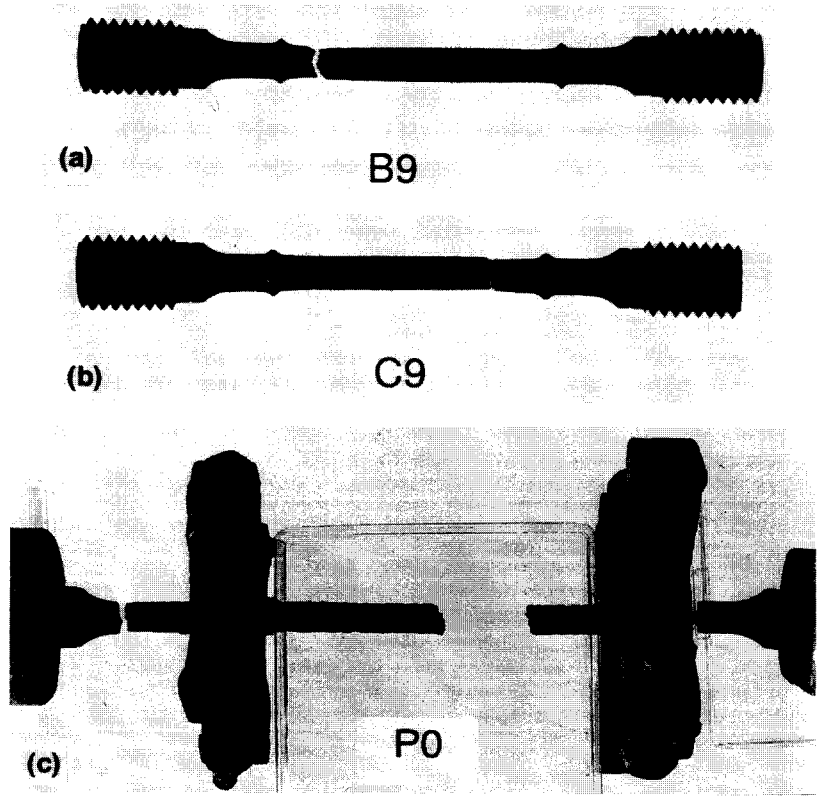


Fig. 9. Optical micrographs of creep-ruptured specimens; (a) specimen with heat treatment B after creep-rupture at 900°C under 39.2 MPa, (b) specimen with heat treatment C after creep-rupture at 900°C under 39.2 MPa and (c) specimen sampled from plates after creep-rupture at 1000°C under 19.6 MPa.

was very brittle due to severe oxidation as shown in Fig. 9(c). This is a typical sample for which anomalous behaviour of creep curves was observed.

Optical micrographs of the creep-ruptured specimen with heat treatment C are shown in Fig. 10. The rupture life of the specimen crept at 900°C under 39.2 MPa was 6865.8 h. Fine precipitates were observed in grain and on grain boundaries. Rupture occurred at grain boundaries where voids formed. Fig. 11 shows optical micrographs of the creep-ruptured specimen sampled from plates. The rupture life of the specimen crept at 1000°C under 19.6 MPa was 9160.4 h and the creep curve exhibited anomalous behaviour as shown in Fig. 8. Oxide clearly forms even at cracks on the grain boundaries of the central regions of the specimen (Fig. 11(b)). Furthermore, coarse precipitates form not only at surface regions but also at central regions.

Fig. 12 shows the SEM micrographs of the creep-ruptured specimen indicated in Fig. 10. In Fig. 12(b) which shows the microstructure of the central region, cracks at the grain boundaries and white precipitates are observed. The fine white precipitates are the $\alpha_2$-W phase containing a large amount of W. Fig. 13 shows the SEM micrographs of the creep-ruptured specimen indicated in Fig. 11. As shown in Fig. 13(a), oxide and cracks form at the grain boundaries from the surface to central regions. Coarse precipitates instead of the fine white precipitates shown in Fig. 12(b) are observed in Fig. 13(b). This coarse precipitate, showing almost the same contrast as that of the matrix, is considered to be the β-Mn type nitride (π

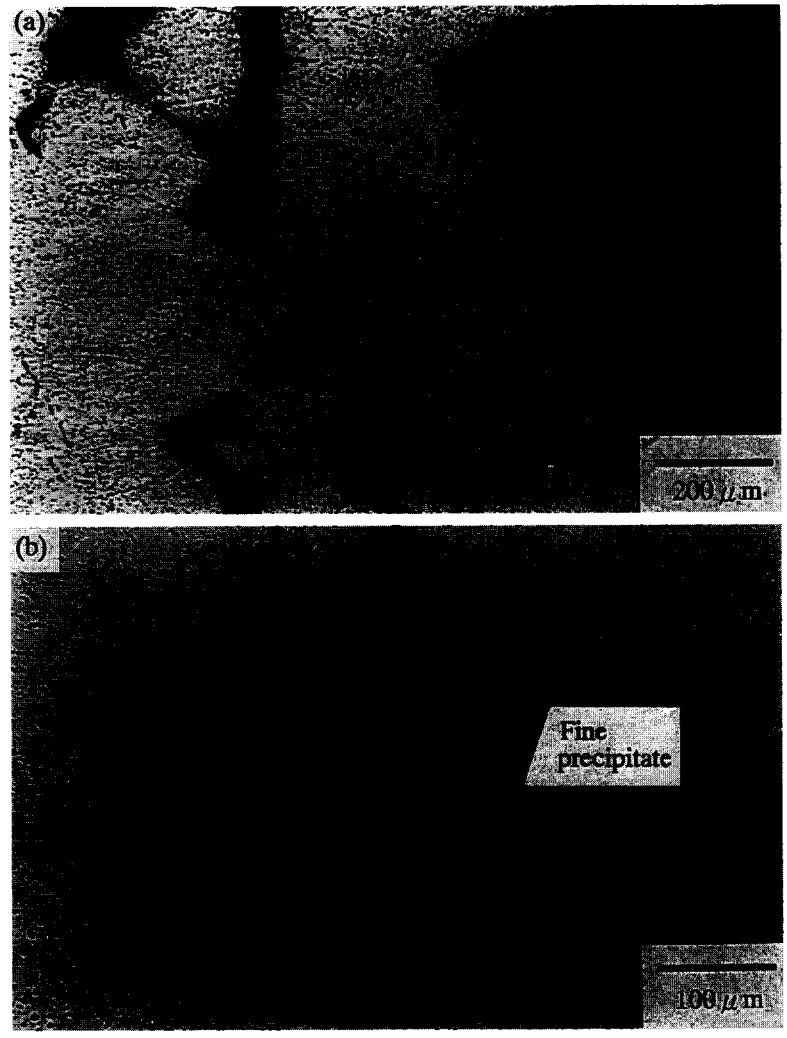


Fig. 10. Microstructures of the creep-ruptured specimen with heat treatment C. Creep test was carried out at 900°C under 39.2 MPa.: (a) ruptured region and (b) central region.

phase) which was found in the creep-ruptured specimen of a Ni–20Cr–20W alloy [10,11].

For this Ni–Cr–W alloy, there are three creep curve types; one normal or classical type and two non-classical types. For the two non-classical types, one is observed at 900°C, the other is observed at 1000°C under low stresses. Primary, secondary and tertiary creep stages exist after the initial low creep rate region in the former case. Sudden rupture occurs during the decrease and steady-state creep rate stages after the tertiary creep stage in the latter case. The latter is the creep curve reported as anomalous creep behaviour where the rupture time increased by a decrease in creep rate after the tertiary creep stage [12–16]. As shown in Fig. 13, this anomalous behaviour is caused by the prevention of crack propagation due to oxide formed at the crack tips on grain boundaries [12–14]. On the other hand, the former non-classical type creep curve is considered to be caused by microstructure change such as precipitation and cell formation during creep.

### 3.3. Analysis of creep rupture data

The time–temperature parameter (TTP) method is often used to analyze creep rupture data and to predict rupture life and stress [17–19]. In the present study, we analyzed the creep rupture data using the Larson–Miller parameter and the Orr–Sherby–Dorn parameter which were typical TTPs.

It is essential to correct creep rupture data of anomalous creep behaviour because the increase in rupture life due to oxide strengthening is only a pretence. Specimens with heat treatment D and sampled from plates exhibited

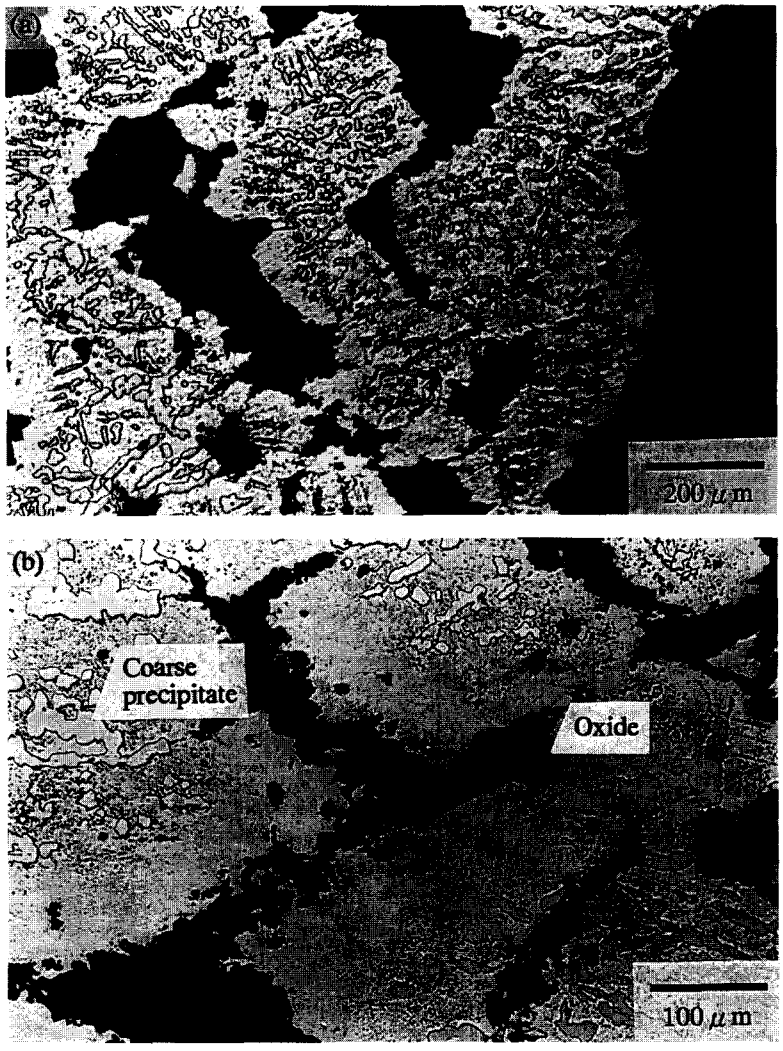


Fig. 11. Microstructures of the creep-ruptured specimen sampled from plates. Creep test was carried out at 1000°C under 19.6 MPa.: (a) ruptured region and (b) central region.

anomalous creep behaviour at 1000°C under 19.6 MPa. Therefore, we corrected these creep curves. An example of correction is shown in Fig. 14. The value of rupture elongation indicated by the cross was obtained from measurement on the reassembled specimen after rupture. The broken pieces were put together and measured using a slide caliper. The creep curve during the tertiary creep stage was drawn by means of manual graphics paying attention to the point that the creep rate increases during the tertiary creep stage.

Rupture lives became half after this correction. We used the following parameters for the corrected data in final TTP analysis.

Larson–Miller:

$$\mathrm{LMP} = T(C + \log t_{\mathrm{R}}), \tag{1}$$

Orr–Sherby–Dorn:

$$\mathrm{OSDP} = \log t_{\mathrm{R}} - Q/19.1425T, \tag{2}$$

where $t_{\mathrm{R}}$ is the time to rupture, $T$ is the absolute temperature and $C$ and $Q$ are parameter constants. Equation $f(\sigma)$,

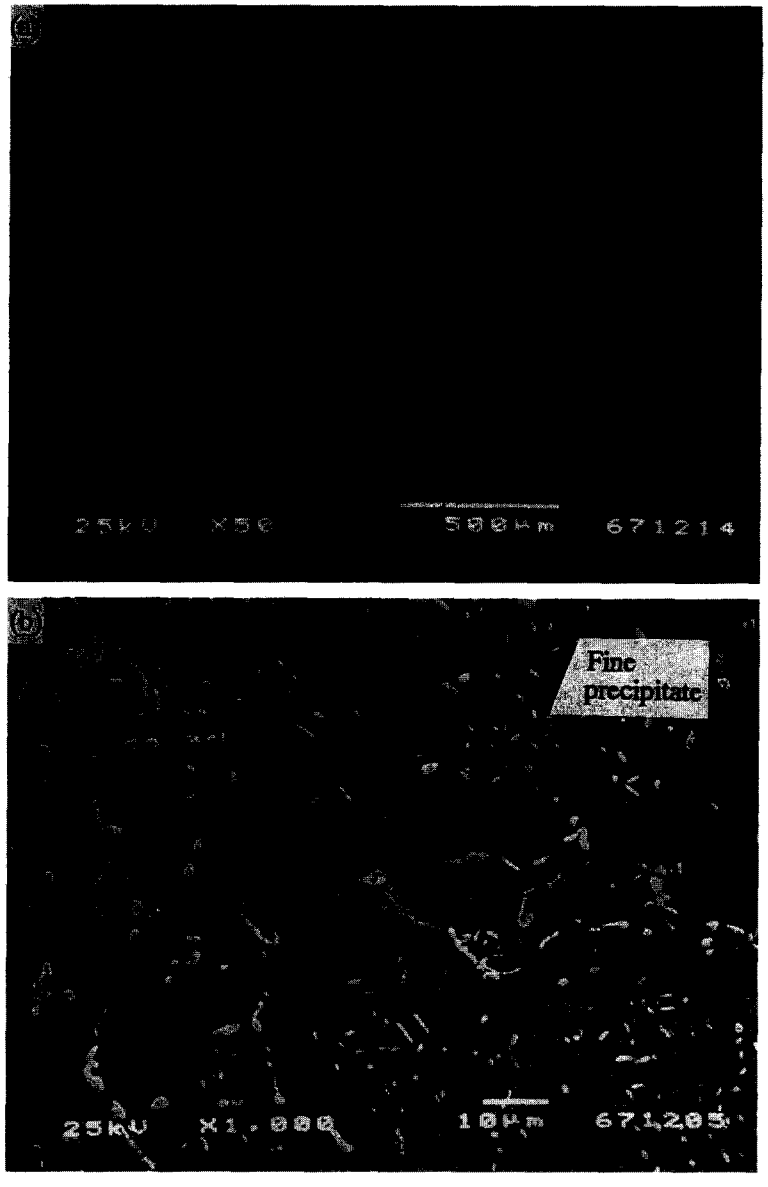


Fig. 12. SEM microstructures of the creep-ruptured specimen with heat treatment C. Creep test was carried out at 900°C under 39.2 MPa.: (a) surface region and (b) central region.

which represents the stress dependence of TTP, is approximated using polynomials of the logarithmic of stress, $\sigma$, as

$$f(\sigma) = b_0 + b_1 \log(\sigma) + b_2(\log(\sigma))^2 + \ldots + b_k(\log(\sigma))^k, \quad (3)$$

where $b_0$, $b_1$, $b_2$, ..., $b_k$ are regression constants. The parameter constants in Eqs. (1)–(3) are optimized to minimize the standard error of estimate (SEE) of log $t_R$.

$$\mathrm{SEE} = \sqrt{\Sigma\left(Y_i - \hat{Y}_i\right)^2 / \left(n_d - n_p - k - 1\right)}, \quad (4)$$

where $Y_i$ is a measured value of log $t_R$, $\hat{Y}_i$ is an estimated value of log $t_R$, $n_d$ is the number of data points, $n_p$ is the number of parameter constant in TTP and $k$ is the degree of Eq. (3). The optimization procedure was carried out following the study on standardization of creep-rupture data evaluation of metals [19].

We calculated Eq. (3) using the degree of polynomials up to 5 and determined the optimum degree using the $F$-test (95% significance). It is found that the degree of polynomials is 1 or 2 for LMP and OSDP to have a good approximation in the case of the Ni–Cr–W alloy. The

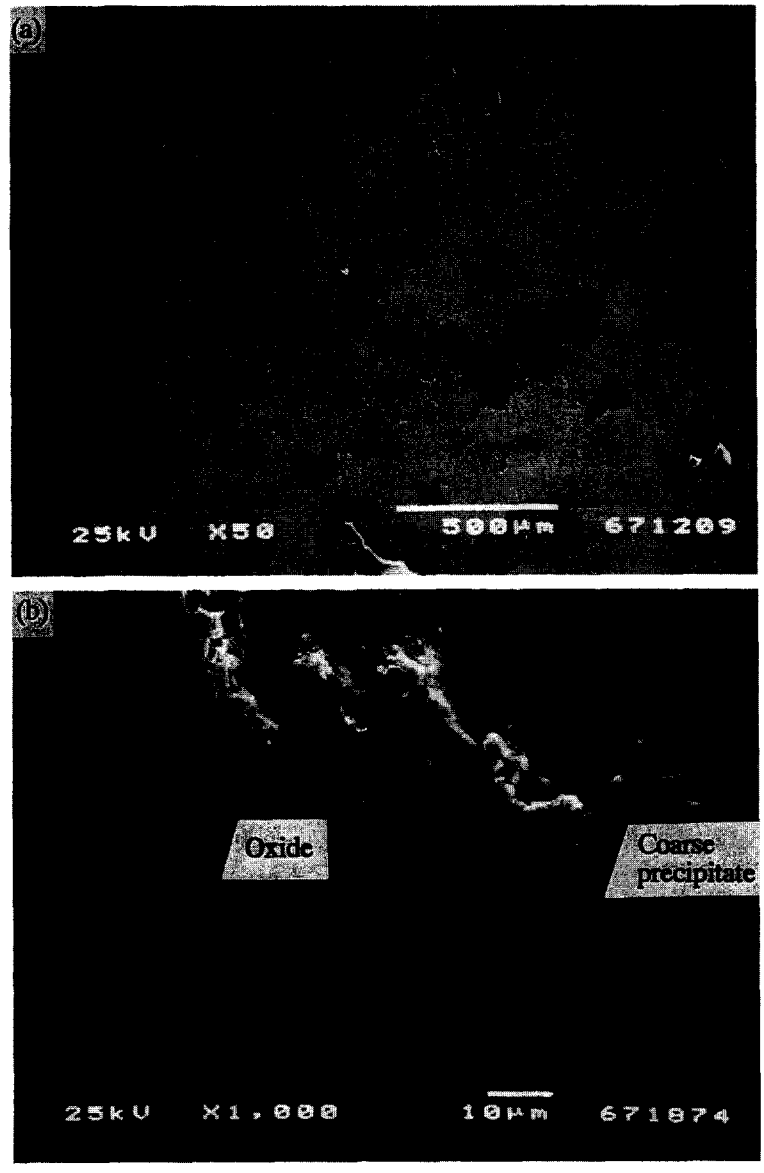


Fig. 13. SEM microstructures of the creep-ruptured specimen sampled from plates. Creep test was carried out at 1000°C under 19.6 MPa.: (a) surface region and (b) central region.

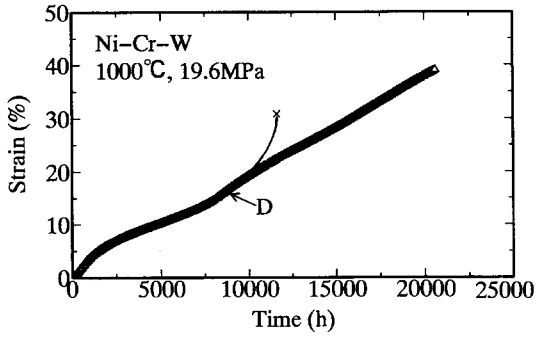


Fig. 14. An example of creep curve corrected for anomalous creep behaviour. The creep test for a Ni–Cr–W alloy with heat treatment D was carried out at 1000°C under 19.6 MPa in air.

application of LMP results in a better fit than that of OSDP since the SEE value for LMP is smaller than that for OSDP. Furthermore, there were some cases where creep rupture strength for a $1 \times 10^5$ h life at 1000°C could not be calculated in a quadratic equation using OSDP. For

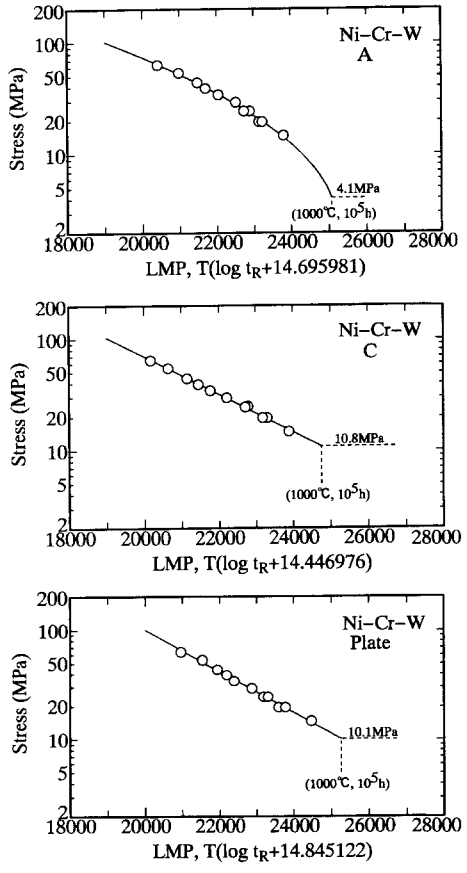


Fig. 15. Relationship between stress and the Larson–Miller parameter (LMP) for specimens with heat treatments A and C and sampled from plates.

Table 3
Results of the Larson–Miller parameter fit for creep rupture times of a Ni–Cr–W alloy

| | Degree | Parameter constants | SEE | Stress for a $1 \times 10^5$ h life at 1000°C (MPa) |
|---|---|---|---|---|
| Heat treatment A | 2 | 14.695981 | 0.064 | 4.1 |
| Heat treatment B | 2 | 15.365570 | 0.071 | 5.5 |
| Heat treatment C | 1 | 14.446976 | 0.057 | 10.8 |
| Heat treatment D | 1 | 17.105267 | 0.128 | 12.2 |
| Plate | 1 | 14.845122 | 0.073 | 10.1 |
| Tube | 2 | 15.344085 | 0.060 | 5.9 |

these reasons, applicability of LMP is better than that of OSDP.

Fig. 15 shows examples of master rupture curves using LMP with predicted values of a $1 \times 10^5$ h life at 1000°C. As shown in the top of Fig. 15, the optimum regression curve for the alloy with heat treatment A is a quadratic equation and the creep rupture strength for a $1 \times 10^5$ h life at 1000°C is 4.1 MPa. The creep rupture strength for a $1 \times 10^5$ h life at 1000°C is 10.8 MPa for the alloy with heat treatment C. The optimum regression curve for corrected data of the samples from plates is a simple equation and the creep rupture strength for a $1 \times 10^5$ h life at 1000°C is 10.1 MPa as shown at the bottom of Fig. 15. Table 3 shows a summary of the optimum regression curves in terms of the Larson–Miller parameter and the predicted value of stress for a $1 \times 10^5$ h life at 1000°C. In Table 3, the calculated values after correction for anomalous creep behaviour are shown for specimens with heat treatment D and sampled from plates. For specimens with heat treatments C and D and sampled from plates, the predicted value of creep rupture strength for a $1 \times 10^5$ h life at 1000°C is clearly above 9.8 MPa which is the final target of the program. Furthermore, we can point out that creep rupture strength increases with increasing heat treatment temperature and grain size.

## 4. Conclusions

Creep rupture properties in an air environment were investigated at 900, 1000 and 1050°C using bar, plate and seamless tube materials of a Ni–Cr–W superalloy developed for use at service temperatures around 1000°C. Long-term creep rupture strength was estimated by applying the time–temperature parameter method to creep rupture data. The results obtained were as follows:

(1) Master rupture curves with optimized parameters for the Ni–Cr–W superalloy were obtained by applying the Larson–Miller parameter method and the Orr–Sherby–Dorn parameter method. The Larson–Miller parameter method is better than the Orr–Sherby–Dorn pa-

rameter method in respect of curve fitting to the present creep-rupture data.

(2) Anomalous creep behaviour where creep rates decrease after the tertiary creep stage is observed in creep curves at 1000°C with rupture times above about 10 000 h. This phenomenon is caused by the suppression of crack propagation due to oxide formed at the crack tips. A correction for this anomalous creep behaviour is presented.

(3) The creep rupture strength for a $1 \times 10^5$ h life at 1000°C was predicted for each material using master rupture curves with optimized parameters. As a result, it is shown that the creep rupture strength of the bar material with grain sizes above ASTM No. 2 and of the plate material is above 9.8 MPa for a $1 \times 10^5$ h life at 1000°C, which is the final target of this program.

(4) The creep rupture strength increases with increasing grain size and heat treatment temperature.

## Acknowledgements

The authors are grateful to the members of the JAERI Subcommittee on Advanced Superalloys (Chairman: Professor emeritus of Tokyo Institute of Technology, R. Tanaka) for their useful discussion and encouragement. Thanks are due to Professor emeritus of the Tokyo Institute of Technology, M. Kikuchi, Professor of the Tokyo Institute of Technology, T. Matsuo and researcher of the National Research Institute for Metals, E. Baba who performed creep tests under contract with JAERI. The authors would like to thank T. Suzuki and S. Kita for their assistance in the microstructure observation and data analysis.

## References

[1] Japan Atomic Energy Research Institute, Present Status of HTGR Research and Development, 1995.
[2] Agency of Industrial Science and Technology–Ministry of International Trade and Industry and the Engineering Research Association of Nuclear Steelmaking, Summary report of R&D project on direct steelmaking technology with high temperature reducing gas-nuclear steelmaking, 1981.
[3] R. Tanaka, T. Matsuo, Tetsu to Hagane 68 (1982) 226.
[4] R. Tanaka, T. Kondo, Nucl. Technol. 66 (1984) 75.
[5] M. Shindo, T. Kondo, Proc. Conf. on Gas-cooled Reactors Today, Vol. 2, Bristol, UK (British Nuclear Energy Society, 1982) p. 179.
[6] Ad Hoc Committee on Advanced Superalloys, Technical Expert Committee on HTGR, Japan Atomic Energy Research Institute, Report JAERI-M 88-270, 1989.
[7] Subcommittee on Advanced Superalloys, Technical Expert Committee on HTGR, Japan Atomic Energy Research Institute, Report JAERI-M 92-137, 1992.
[8] H. Tsuji, H. Nakajima, T. Kondo, Proc. Int. Conf. on Materials for Advanced Power Engineering, Liège, Belgium, 1994, pp. 939–948.
[9] H. Tsuji, M. Ohashi, M. Takemura, H. Nakajima, Japan Atomic Energy Research Institute, Report JAERI-M 92-148, 1992.
[10] T. Matsuo, K. Ohmura, R. Tanaka, Tetsu to Hagane 71 (1985) 1009.
[11] M. Kikuchi, S. Wakita, R. Tanaka, Trans. Iron Steel Inst. Jpn. 13 (1973) 226.
[12] National Research Institute for Metals, Report No. 3, 1982, p. 120.
[13] T. Itagaki, T. Watanabe, R. Yoda, Nihon-Kinzoku-Gakkai Shi 40 (1976) 914.
[14] R. Widmer, N.J. Grant, Trans. ASME 82 (1960) 882.
[15] P. Shahinian, Trans. ASM 49 (1957) 862.
[16] P. Shahinian, M.R. Achter, Trans. ASM 51 (1959) 244.
[17] Task Group, Subcommittee on Extrapolation of Creep-Strength, The Research Committee on High-Temperature Strength of Materials, Manual on the Extrapolation Methods of Creep-Rupture Data in Accordance with ISO 6303, Iron and Steel Institute of Japan, 1983.
[18] R. Viswanathan, Damage Mechanism and Life Assessment of High-Temperature Components (ASM International, Metals Park, OH, 1989).
[19] VAMAS Data Evaluation Committee, Study on Standardization of Creep-Rupture Data Evaluation of Metals, Iron and Steel Institute of Japan, 1994.